Proc. International Conference on Mechanical, Automotive and Mechatronics Engineering (ICMAME 2023)
29-30 April 2023, Dubai, UAE

Numerical Investigation of Transition Turbulence Model for Turbine Airfoil at Low Reynolds Number

Mohamed Atef
Mechanical Power Engineering Dept. Faculty of Engineering,
The British University in Egypt
Cairo, Egypt
Pg.Mohamed92010032@bue.edu.eg

Ahmed El Baz
Mechanical Power Engineering Dept. Faculty of Engineering,
The British University in Egypt
Cairo, Egypt
ahmed.elbaz@bue.edu.eg

***Abstract*— The transition towards a greener energy future has spurred a growing interest in wind energy as a reliable and clean alternative to conventional energy sources. To optimize wind turbine performance, it is crucial to understand the aerodynamics of wind turbines at different Reynolds numbers. In this study, we use the (γ−$\tilde{R}$ $e\theta$) transition model to investigate the performance of Vertical Axis Wind Turbines (VAWTs) at low Reynolds numbers. Specifically, we employ a NACA0018 airfoil and two-dimensional Reynolds-Averaged Navier-Stokes (RANS) equations, along with optimized meshing and solver settings in ANSYS Fluent. We validate our model by simulating wind turbine performance at Reynolds numbers of 500k and 700k and various angles of attack and comparing our results with experimental data from two wind tunnel studies reported in the scientific literature. Our findings show good agreement between the numerical and experimental results, providing useful insights into the behavior of VAWTs at low Reynolds numbers. By conducting the study in 2D, we optimize computational cost and iteration time while still providing valuable data for future 3D modelling efforts. This study contributes to our understanding of wind turbine aerodynamics and could inform the development of more efficient wind turbines for a sustainable energy future.**

Keywords*— *NACA-0018 airfoil, RANS solver, Transition Turbulence Modelling, Low Reynolds number airfoils turbine, CFD

I. INTRODUCTION

The use of wind energy in various forms, such as small scale wind turbines and modern airship propulsion systems, requires the use of low Reynolds number airfoils. This has prompted researchers to concentrate on examining the performance of airfoil turbines at different Reynolds numbers [1].

Different methods have been developed to study the aerodynamic behavior of airfoils at varying Reynolds numbers. One such method is experimental modelling, which involves building small-scale models and using the results to inform larger scale turbines. However, despite advancements in precision and accuracy, this approach still faces challenges in terms of cost and availability of facilities. Another approach is computational modelling using techniques such as Computational Fluid Dynamics (CFD), which is widely used in the wind industry. CFD eliminates the need for complex experimental setups but still requires high computational power, such as High-Performance Computing (HPC), for simulating intricate models. On the other hand, CFD provides a wider range of data compared to experimental methods once the simulation is complete.

The flow regime near the wall at low Reynolds numbers is influenced by the curvature of the airfoil surface, causing a reduction in flow speed and lower kinetic energy, leading to a laminar layer separation. [2].

The transition from laminar to turbulent flow has been studied through experimental techniques for symmetrical airfoils such as the NACA 0018 by examining the lift coefficient at different angles of attack [3]. The studies by Damiola et al. [4] and Boutilier and Yarusevych [5] both focused on measuring the flow around a NACA-0018 airfoil at low Reynolds numbers. They used different parameters such as surface pressure and velocity to understanded the aerodynamic characteristic and performance of symmetrical airfoils.

The ability of turbulence models to identify early transition is crucial for understanding the early stall phenomenon, which leads to a rapid increase and drop in the drag and lift coefficients respectively. The (γ−$\tilde{R}$ $e\theta$) turbulence transition model which has been introduced by Menter et al. [6] uses an empirical correlation for transition prediction.

There have been various numerical studies delivered based on (γ−$\tilde{R}$ $e\theta$) model and have demonstrated the model's ability and accuracy to understand the airfoil aerodynamics. For example, Khayatzadeh et al. [7] simulation based on the turbulence transition for two different wind turbine profiles at Re > 2 * 10^6, and verified the results with the modelled lift, drag, and moment coefficients. M. A. A. Bari et al. [8] calibrated the intermittency transition turbulence model utilizing machine learning algorithm. Kapsalis et al. [9] compared K–V turbulence transition model and additional two transition models which showed that K-V model has the capability in predicting NACA 0012 performance against the experimental results.

Morgado et al. [10] demonstrated the (k-kl-ω) transition model being more robust at low Reynolds numbers in comparison with the fully turbulent (k-ω) SST model.

Al Orabi et al. [11] attempted to reproduce the results of wind tunnel experiments using the (γ−$\tilde{R}$ $e\theta$) transition model in open field and wall-bounded domains with dimensions matching the wind tunnel to evaluate the impact of boundary conditions on the model's outcome.

The ($\gamma-\tilde{R}\ e\theta$) constants have been updated and verified at various flow conditions; test cases with both zero and non-zero pressure gradients, making it a suitable choice for the current study [12].

II. THE COMPUTATIONAL MODEL

A. The Computational Domain

The selection of an appropriate domain boundary and the definition of accurate boundary conditions are crucial in building a reliable and accurate CFD model. It is essential to define the velocities, pressures, and temperatures at the boundaries of the computational domain as they have a direct impact on the results of the simulation. The size and shape of the computational domain also play a crucial role in determining the computational cost and accuracy of the simulation. Therefore, it is important to choose it judiciously, ensuring that it captures the essential physics of the problem while keeping its complexity to a minimum. In this study, a C-type domain was selected for the simulation, as it reduces the size of the computational domain and decreases the computational cost [13]. Moreover, it allows for changes in the Angle of Attack (AoA) by simply editing the inlet velocity components based on the corresponding AoA, without the need to modify the mesh.

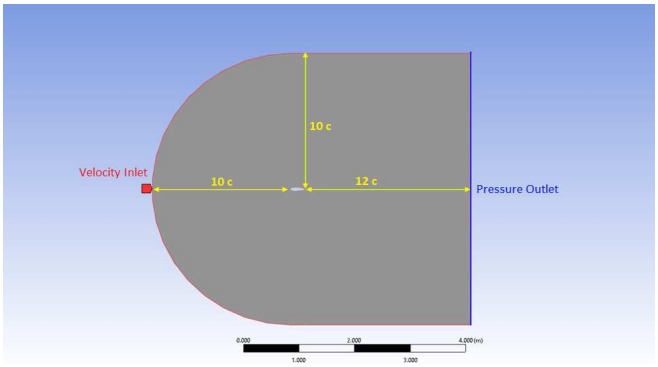

Fig. 1. Domain with respect to Chord length (C)

B. Mesh Generation

The second step involved dividing the domain into five zones using a mapped mesh and adjusting element sizes using a biased factor. This allowed for increased element sizes near the domain boundary and decreased sizes near the airfoil and railing edge wall to capture flow transitions, achieving a balance between computational cost and accuracy in the simulation.

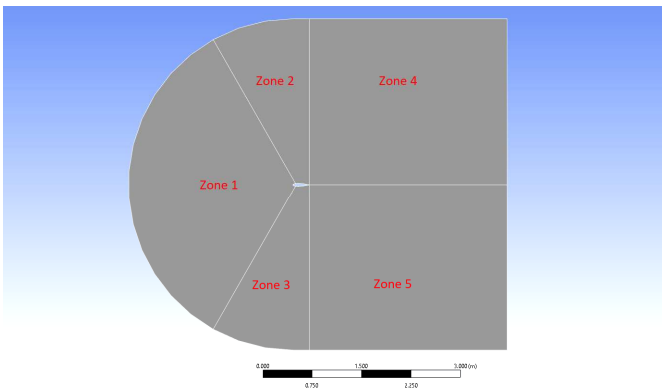

Fig. 2. Model Domain Zonation

To produce a high-quality mesh for an airfoil simulation, multiple iterations were performed to keep y-plus below 1 [14]. The mesh used a quadrilateral model to ensure each element was as close as possible to its optimal shape and a skewness value less than 0.6 for numerical stability and accuracy. The aspect ratio was also maintained below 10 near the airfoil wall. The goal was to attain all these criteria for a high-quality mesh while avoiding excessive computational costs by not creating an overly fine model. For industrial-scale models, a finer mesh may lead to higher computational costs but will reduce the time needed to meet the key criteria for a stable and reliable model. Commercial software like ANSYS Icem can also be used to improve mesh quality.

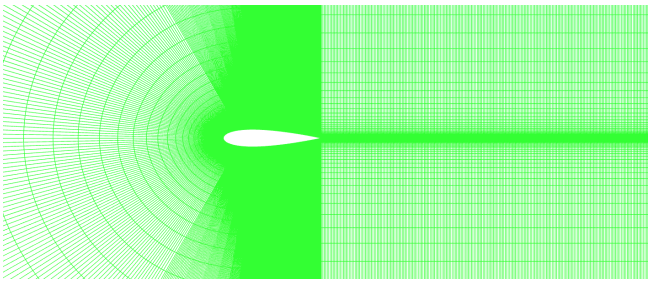

Fig. 3. Model Mesh Zoom out

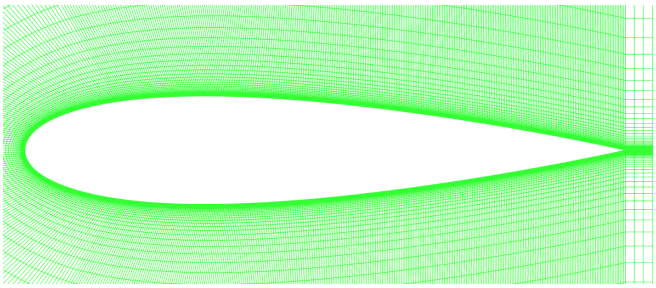

Fig. 4. Model Mesh – Zoom in (Near wall)

C. Solver Settings

Adjust the settings in the Ansys Fluent solver to make sure the proper parameters are included in the model. For this project, the Steady state, pressure based coupled solver was chosen. The density of air and dynamic viscosity were set at 1.225 [kg/m3] and 1.7894 10-5 [Pa s], respectively. The inlet velocity component was modified according to the simulated angle of attack, with a turbulent intensity of 0.1% and a turbulent viscosity ratio of 10 [15]. A turbulence intensity of 0.1% is a common value for low-turbulence wind tunnel simulations and a lower value indicates a natural or separation-induced transition mechanism. The turbulent viscosity ratio is the ratio of turbulent viscosity to molecular viscosity and a value of 10 is typical for low-turbulence wind tunnel simulations. A lower value of the turbulent viscosity ratio means a higher level of turbulence in the flow.

To start with, the stability of the model was evaluated using the first order upwind scheme, but the results were ultimately based on second order upwind methods for pressure, momentum, and turbulence. To achieve more accurate results, a least squares cell-based scheme was employed for gradient spatial discretization. The objective was to obtain a residual value of less than 10^{-05} for all equations. As the angle of attack increased, especially beyond stall, it required more iterations to reach the desired residual level.

D. *Turbulence Model*

The SST (Shear Stress Transport) transition model, also known as the ($\gamma-\tilde{R}\ e\theta$) transition model, is a Reynolds-averaged Navier-Stokes (RANS) turbulence model that is available in ANSYS Fluent. This advanced turbulence model predicts the transition from laminar to turbulent flow and the behavior of the turbulent boundary layer on airfoils. It is based on the Reynolds-averaged Navier-Stokes equations and features a transport equation for the turbulent shear stress, which enables it to model the transition from laminar to turbulent flow. The formulation proposed by Menter et al. [6,12] is based on the widely utilized (k-ω) SST model but includes two extra transport equations. The first equation, called the intermittency (γ) equation, is used to initiate the transition process, while the second equation is related to the transition onset Reynolds number ($\tilde{R}\ e\theta$). These transport equations are driven by experimental correlations rather than modelling the underlying physics of transition. As a result, this model is suitable for any type of transition mechanism but only if the correct parameters are provided through accurate calibration [16].

The SST model employs a blending function that seamlessly merges the laminar and turbulent regions of the flow, and it also includes a transport equation for the turbulent boundary layer thickness. Compared to the standard k-epsilon and k-omega models, the SST model is considered a more advanced turbulence model. It provides accurate predictions of the turbulent boundary layer on airfoils and is widely used in the aerospace industry.

III. Results and Discussion

The NACA-0018 airfoil's flow was analyzed and predicted at Reynolds numbers of 500k and 700k for various angles of attack (AOA) ranging from 0 to 24 degrees, using the transition model. The results of the predictions were compared with experimental data that measured aerodynamic forces such as lift and drag coefficients, as well as the pressure distribution on the surface and skin friction coefficient.

Figures 5 and 6 display the change in lift and drag coefficients at 500k Reynolds, and their comparison to experimental data. The results show a strong correlation with the measured values. The study by Timmer observed significant post-stall hysteresis loops, resulting in a significant decrease in lift, which is also apparent in the current results. The model's prediction of the drag coefficients before stall aligns with Timmer's findings [17], but it fails to capture the onset of free transition until around 22 degrees of leading edge stall angle.

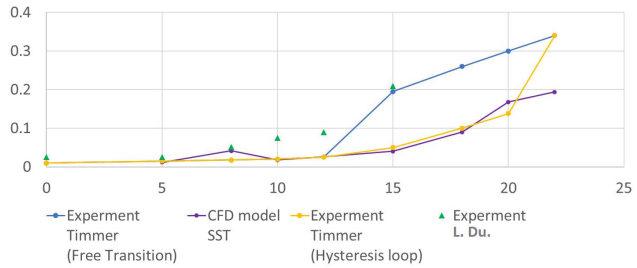

Fig. 5. Drag Coefficient at 500k Re

In contrast, there was a major discrepancy between Timmer's results and those of M. S. H. Boutilier et al. until 15 degrees, but then the free transition drag coefficient matched. Notably, at an angle of attack of 8 degrees, the model aligned with the drag coefficient measured by L. Du. [18].

The calculated lift coefficient agreed with Timmer's measured lift coefficient until stall onset at around 12 degrees [17]. Afterward, the lift coefficient gradually decreased over the next 10 degrees until it reached 22 degrees where both hysteresis and free transition flow were equal. The current model significantly underestimates lift and drag coefficients, and this discrepancy becomes greater as the angle of attack increases until reaching the maximum leading-edge stall angle of 22 degrees.

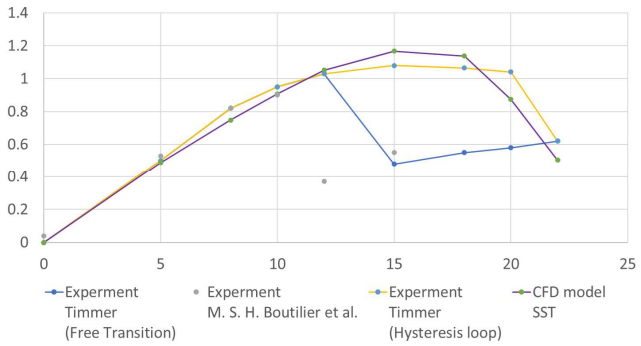

Fig. 6. Lift Coefficient at 500k Re

The model was thoroughly tested and evaluated by applying it at a higher Reynolds number of 700k and comparing the results to the experimental data. The comparison revealed a good match between the model's predicted lift coefficient and the measured lift coefficient at a Reynolds number of 500k. The same was observed for the drag coefficient.

However, Analysis showed increased Reynolds number increases hysteresis loop length. This discovery necessitated an extension of the modelling process to 24 degrees at the 700 Re due to complexity of the flow behavior.

The lift and drag coefficients produced by the model were found to be in close agreement with the results of the Timmer experiment. The correlation between the model and the experiment is illustrated in Figures 7 and 8, which show the lift coefficient and drag coefficient, respectively. The match between the model and the experiment was strong until around 12 degrees, after which the lift coefficient declined to its lowest point at 22 degrees before gradually increasing.

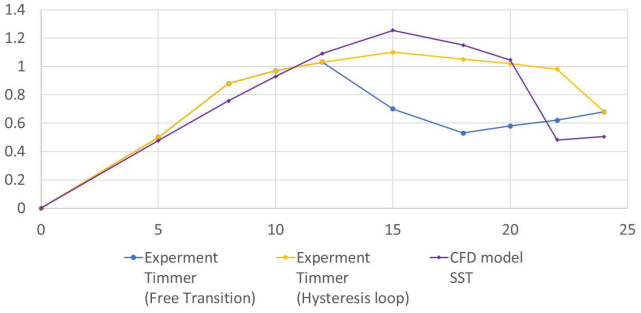

Fig. 7. Lift Coefficient at 700k Re

The lift and drag coefficients predicted by the current model are not quite accurate, with the error becoming more

noticeable as the angle of attack increases, reaching a peak at around 22 degrees.

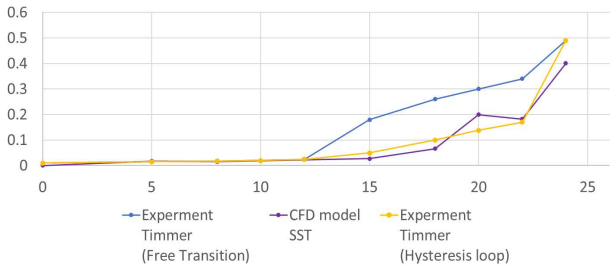

Fig. 8. Drag Coeffiecent at 700 Re

Before the stall angle, The flow over the airfoil creates a peak suction pressure which decreases due to wall shear stress, forming a laminar separation bubble. A strong pressure recovery occurs before the flow reattaches and becomes turbulent again. The pressure plateau indicates the separation (S), transition (T), and reattachment (R) points [19].

The pressure distribution along the surface of an airfoil can provide valuable information about the flow behaviour and aerodynamic performance. The separation point is a critical stage in the flow, as it marks the point where the flow separates from the surface and forms a laminar separation bubble. This leads to a drop in pressure and affects the lift generated by the airfoil. The transition point is another important stage, where the flow transitions from laminar to turbulent. This is often associated with a sharp drop in pressure and a change in the flow pattern.

The reattachment point is where the flow reattaches to the surface of the airfoil after having separated. It is identified by a linear drop in pressure downstream of the airfoil. This stage marks the end of the laminar separation bubble and the return to a more stable flow pattern. The pressure distribution along the airfoil can be used to determine the lift, drag, and other aerodynamic coefficients.

When an airfoil exceeds its stall angle, it is deemed to be in a fully stalled state, which causes a significant alteration in the pressure distribution. The airflow becomes more turbulent and the pressure distribution becomes more intricate, making it challenging to anticipate the aerodynamic performance of the airfoil beyond the stall angle. This can lead to a loss of lift and instability, emphasizing the significance of preventing or minimizing stalling in the design of aircraft.

Comprehending the pressure distribution across the airfoil is of utmost importance in the development and enhancement of aircraft and other aerodynamic equipment. It imparts valuable insights into the flow characteristics, such as the creation and behavior of the laminar separation bubble, the transition point, and the reattachment point. Such knowledge can be applied to ameliorate the aerodynamic effectiveness, stability, and safety of aircraft and other aerodynamic devices.

This study modeled both the skin friction coefficient and pressure coefficient at a Reynolds number of 500k and various angles of attack from 0 to 15 degrees. To simplify the identification of the separation point (S), transition point (T), and reattachment point (R), both parameters were displayed in the same graph for each angle of attack, figures 9 - 11. At the onset of transition, the skin friction coefficient rapidly increases and practically, the wall shear stress produced by the boundary layer fades away at an inflection point due to a change in flow direction [21]. By using this technique on the plotted skin friction coefficient and pressure coefficient along the airfoil suction side, the separation point, transition point, and reattachment point can be determined accurately.

we can see that as the angle of attack (AOA) of the airfoil rises up to the stall angle, the suction pressure rises as well. However, after the stall, the pressure distribution on the airfoil's suction side changes because of the burst of the separation bubble, leading to no reattachment, which results in a significantly lower maximum suction pressure for AOA=15 compared to AOA=8. As the angle of attack increases, the separation point on the airfoil moves closer to the leading edge and the size of the separation bubble decreases. This is a common occurrence for airfoils operating at low Reynolds numbers, as stated in references [20]

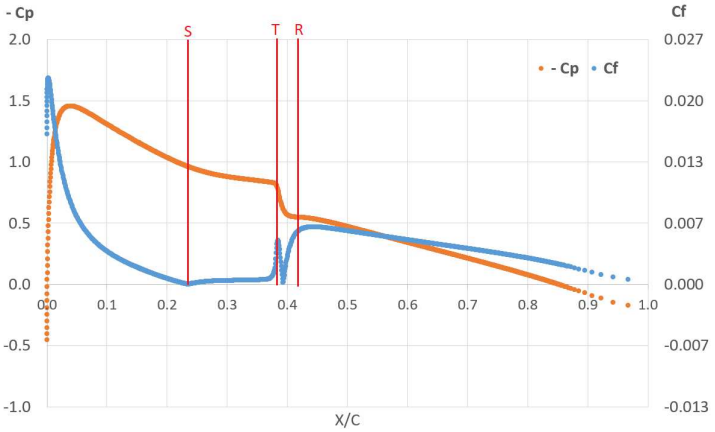

Fig. 9. - Cp and Cf at Re 500k and AoA 5deg across the airfoil suction side. Red lines: Separation (S), Transition (T) and Reattachment (R)

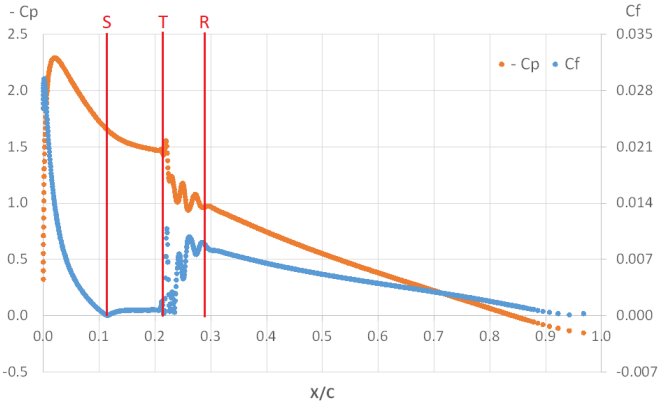

Fig. 10. - Cp and Cf at Re 500k and AoA 8deg across the airfoil suction side. Red lines: Separation (S), Transition (T) and Reattachment (R)

In essence, the flow over an airfoil surface begins with the skin friction at its maximum value as the free stream catches the leading edge. (S) marks the decrease in wall shear stress and skin friction, (T) marks the rapid increase in skin

friction, (R) marks the end of reverse flow. (T.S) marks another minimum in skin friction, indicating turbulent separation at the trailing edge [21].

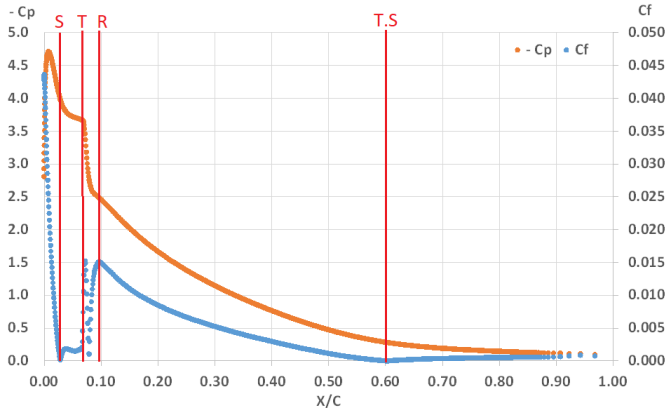

Fig. 11. - Cp and Cf at Re 500k and AoA 15deg across the airfoil suction side. Red lines: S, T, R, and (T.S) Turbulent Separation

IV. Conclusion

In this study, we conducted a comprehensive computational simulation of the transitional flow over a NACA-0018 airfoil at Reynolds numbers of 500k and 700k, with various angles of attack. We used the steady flow equations with the (γ–$\tilde{Re}\theta$) transition model to accurately model the flow behavior from laminar to turbulent. Our optimized boundary domain, grid, and numerical methods ensured accurate results, which were validated by good agreement between computational and experimental data at free transition.

Our study identified the skin friction coefficient as a more reliable indicator of separation, transition, and reattachment locations compared to the surface pressure coefficient. This finding highlights the importance of considering multiple flow parameters when analysing transitional flow behaviour and can inform future research on airfoil performance.

Overall, our results provide insights that can improve our understanding of transitional flow behaviour and inform the development of more accurate computational models for predicting airfoil performance.

References

[1] M. Rong, Z. B. Wen, and L. P. Qing, “Optimization design study of low-Reynolds-number high-lift airfoils for the high-efficiency propeller of low-dynamic vehicles in stratosphere,” Sci. China Technol. Sci., vol. 53, no. 10, pp. 2792–2807, 2010, doi: 10.1007/s11431-010-4087-0.

[2] H. Schlichting and K. Gersten, “Boundary-Layer Theory,” Boundary-Layer Theory, pp. 1–799, 2016, doi: 10.1007/978-3-662-52919-5.

[3] W. A. Timmer, “Two-dimensional low-Reynolds number wind tunnel results for airfoil NACA 0018,” Wind Eng., vol. 32, no. 6, pp. 525–537, 2008, doi: 10.1260/030952408787548848.

[4] L. Damiola, M. F. Siddiqui, M. C. Runacres, and T. D. Troyer, “Influence of free-stream turbulence intensity on static and dynamic stall of a NACA 0018 aerofoil,” J. Wind Eng. Ind. Aerodyn., vol. 232, no. 105270,2023, doi: 10.1016/j.jweia.2022.105270.

[5] M. S. H. Boutilier and S. Yarusevych, “Effects of end plates and blockage on low-Reynolds-number flows over airfoils,” AIAA J., vol. 50, no. 7, pp. 1547–1559, 2012, doi: 10.2514/1.J051469.

[6] F. R. Menter, R. B. Langtry, S. R. Likki, Y. B. Suzen, P. G. Huang, and S. Völker, “A correlation-based transition model using local variables - Part I: Model formulation,” J. Turbomach., vol. 128, no. 3, pp. 413–422, 2006, doi: 10.1115/1.2184352.

[7] Khayatzadeh, P., Nadarajah, “S.: Laminar-turbulent flow simulation for wind turbine profiles using the c–Reht transition model,” Wind Energy 17, 901–918 (2014).

[8] M. A. A. Bari, A. D. Ronch, M. Panzeri, J. Drofelnik, “On the calibration of the intermittency transiton turblence model for wind turbine air foil by machine learning algorithm” ICAS, 31st, 2018.

[9] P. C. S. Kapsalis, S. Voutsinas, and N. S. Vlachos, “Comparing the effect of three transition models on the CFD predictions of a NACA0012 airfoil aerodynamics,” J. Wind Eng. Ind. Aerodyn., vol. 157, pp. 158–170, 2016, doi: 10.1016/j.jweia.2016.07.007.

[10] J. Morgado, R. Vizinho, M. A. R. Silvestre, and J. C. Páscoa, “XFOIL vs CFD performance predictions for high lift low Reynolds number airfoils,” Aerosp. Sci. Technol., vol. 52, pp. 207–214, 2016, doi: 10.1016/j.ast.2016.02.031.

[11] M. Y. Al Orabi, A. M. R. Elbaz, N. A. Mahmoud, and A. M. Hamed, “Computational modeling of transitional flow over NACA-0018 airfoil at low Reynolds Number,” International Journal of Advance Research, Ideas and Innovations in Technology, Vol. 6, no. 6.

[12] R. B. Langtry, F. R. Menter, S. R. Likki, Y. B. Suzen, P. G. Huang, and S. Völker, “A correlation-based transition model using local variables - Part II: Test cases and industrial applications,” J. Turbomach., vol. 128, no. 3, pp. 423–434, 2006, doi: 10.1115/1.2184353.

[13] S. Mauro, R. Lanzafame, M. Messina, and D. Pirrello, “Transition turbulence model calibration for wind turbine airfoil characterization through the use of a Micro-Genetic Algorithm,” Int. J. Energy Environ Eng., vol. 8, pp. 359–374, 2017.

[14] R. B. Langtry, J. Gola, and F. R. Menter, “Predicting 2D Airfoil and 3D Wind Turbine Rotor Performance using a Transition Model for General CFD Codes,” Sci. York, vol. 2006, no. January, pp. 1–11, 2006.

[15] R. Langtry, and F. Menter, “Transition Modeling for General CFD Applications in aeronautics,” AIAA, 43rd, 2005-522.

[16] R. Langtry, F. Menter, and S. Volker, “Transition modelling for general purpose CFD codes,” Flow Turb. Combust., Vol. 77, pp. 277–303, 2006.

[17] W. A. Timmer, “Two-dimensional low-reynolds number wind tunnel results for airfoil NACA0018,” Wind Eng., Vol. 32, no. 6, pp. 525–537, 2008.

[18] L. Du, “Numerical and Experimental Investigations of Darrieus Wind Turbine Start-up and Operation,” PQDT - UK Irel., 2015.

[19] M. S. H. Boutilier and S. Yarusevych, “Parametric study of separation and transition characteristics over an airfoil at low Reynolds numbers,” Exp. Fluids, vol. 52, no. 6, pp. 1491–1506, 2012, doi: 10.1007/s00348-012-1270-z.

[20] M. M. O’Meara and T. J. Mueller, “Experimental Determination of the Laminar Separation Bubble Characteristics of an Airfoil At Low Reynolds Numbers.,” AIAA Pap., vol. 25, no. 8, 1986, doi: 10.2514/6.1986-1065.

[21] P. K. Kundu, I. M. Cohen, and D. R. Dowling, Boundary Layers and Related Topics. 2016.